Thermo-Optical Arrays of Flexible Nanoscale Nanomembranes Freely Suspended over Microfabricated Cavities as IR Microimagers

Chaoyang Jiang,[†] Michael E. McConney,[†] Srikanth Singamaneni,[†] Emily Merrick,[†] Yuchuan Chen,[‡] Jing Zhao,[‡] Lei Zhang,[‡] and Vladimir V. Tsukruk*,[†]

Department of Materials Science and Engineering, Iowa State University, Ames, Iowa 50011, and Agiltron Incorporated, Woburn, Massachusetts 01801

Received February 19, 2006
Revised Manuscript Received April 3, 2006

Robust and flexible nanocomposite membranes have received increasing attention as a result of their unique micromechanical properties critical for prospective applications in microsensor technologies.[1−7] These flexible free-standing membranes are considered as prospective sensing elements in ultrasensitive mechanical, optical, and biological sensors and are extremely suitable for the assembly into lightweight and portable devices. [8−11] With the introduction of microelectromechanical systems technology, traditional sensors are being reinvented in a miniaturized form, such as Golay photothermal cells,[12] which are based on pneumatically mediated membrane deflections[13−15] Layer-by-layer (LbL) assembly, which facilitates the fabrication of versatile multilayer structures,[16−18] has been successfully used to fabricate a variety of nanoscale composite membranes with an overall thickness ranging from several nanometers to micrometers.[19−22]

In recent studies, we demonstrated that spin-assisted LbL assembly is a fast and versatile fabrication technique leading to nanoscale (with a thickness 20−60 nm) freely suspended composite membranes with encapsulated gold nanoparticles and carbon nanotubes.[23−25] Micropatterning of various nanostructures inside the nanomembranes has been achieved.[26] The micromechanical behavior of membranes freely suspended over openings with different diameters was studied, and the elastic moduli in the range 2−8 GPa have been reported.[27]

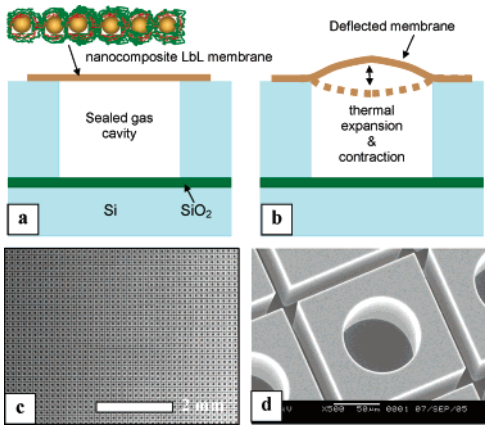

Figure 1. Photothermal sensitive arrays and SEM micrographs of microfabricated cavities: (a, b) Cartoons of a microcavity sealed with a freely suspended nanomembrane in the planar state at room temperature (a) and in deformed states (b); (c) SEM micrograph of the silicon substrate with a uniform array of microcavities; and (d) higher magnification SEM image showing the smooth edges of the microcavity and the trenches separating the individual cavities.

However, there are several critical aspects that should be addressed to employ these nanomembranes for photothermal sensing and imaging applications. First, a direct photothermal phenomenon (like that observed for photothermal Golay cells) has not been demonstrated for a single photothermal cell sealed with the nanomembrane (Figure 1). Second, their ability for fast, reproducible, sensitive, and uniform response to external thermal stimuli (thermal flux and IR laser illumination) should be demonstrated. Only direct demonstration of these abilities will open the door for miniature, photothermal cell arrays with microthermal imaging with high sensitivity and versatility.

In this communication, we report the photothermal phenomenon for a single microscopic (80 μm across) cavity

* To whom correspondence should be addressed. E-mail: vladimir@iastate.edu.
[†] Iowa State University.
[‡] Agiltron Incorporated.

(1) Mamedov, A. A.; Kotov, N. A.; Prato, M.; Guldi, D. M.; Wicksted, J. P.; Hirsch, A. *Nat. Mater.* **2002**, *1*, 190.
(2) Jiang, C.; Markutsya, S.; Pikus, Y.; Tsukruk, V. V. *Nat. Mater.* **2004**, *3*, 721.
(3) Nolte, A. J.; Rubner, M. F.; Cohen, R. E. *Macromolecules* **2005**, *38*, 5367.
(4) Nolte, M.; Schoeler, B.; Peyratout, C. S.; Kurth, D. G.; Fery, A. *Adv. Mater.* **2005**, *17*, 1665.
(5) Jiang, C.; Tsukruk, V. V. *Adv. Mater.* **2006**, *18*, 829.
(6) Tong, H. D.; Jansen, H. V.; Gadgil, V. J.; Bostan, C. G.; Berenschot, E.; van Rijn, C. J. M.; Elwenspoek, M. *Nano Lett.* **2004**, *4*, 283.
(7) Hashizume, M.; Kunitake, T. *Soft Matter* **2006**, *2*, 135.
(8) Lutkenhaus, J. L.; Hrabak, K. D.; McEnnis, K.; Hammond, P. T. *J. Am. Chem. Soc.* **2005**, *127*, 17228.
(9) Brott, L. L.; Rozenzhak, S. M.; Naik, R. R.; Davidson, S. R.; Perrin, R. E.; Stone, M. O. *Adv. Mater.* **2004**, *16*, 592.
(10) Gheith, M. K.; Sinani, V. A.; Wicksted, J. P.; Matts, R. L.; Kotov, N. A. *Adv. Mater.* **2005**, *17*, 2663.
(11) Eck, W.; Küller, A.; Grunze, M.; Völkel, B.; Gölzhäuser, A. *Adv. Mater.* **2005**, *17*, 2583.
(12) Agnew, J. T. *Trans. ASME* **1949**, *71*, 107.
(13) Janes, J. *Ger. Offen.* **1997**, DE 19523526.
(14) Yamashita, K.; Murata, A.; Okuyama, M. *Sens. Actuators A* **1998**, *66*, 29.
(15) Hazel, J.; Fuchigami, N.; Gorbunov, V.; Schmitz, H.; Stone, M.; Tsukruk, V. V. *Biomacrolecules* **2001**, *2*, 304.
(16) (a) Decher, G., Schlenoff, J. B., Eds.; *Multilayer Thin Films*; Wiley-VCH: Weinheim, Germany, 2003. (b) Hammond, P. T. *Adv. Mater.* **2004**, *16*, 1271. (c) Li, J.; Möhwald, H.; An, Z.; Lu, G. *Soft Matter* **2005**, *1*, 259.
(17) Johnston, A. P. R.; Read, E. S.; Caruso, F. *Nano Lett.* **2005**, *5*, 953.
(18) Shi, X.; Shen, M.; Möhwald, H. *Prog. Polym. Sci.* **2004**, *29*, 987.
(19) (a) Vinogradova, O. I. *J. Phys.: Condens. Matter* **2004**, *16*, R1105. (b) Angelatos, A. S.; Katagiri, K.; Caruso, F. *Soft Matter* **2006**, *2*, 18. (c) Zhai, L.; Cebeci, F. C.; Cohen, R. E.; Rubner, M. F. *Nano Lett.* **2004**, *4*, 1349.
(20) Mallwitz, F.; Laschewsky, A. *Adv. Mater.* **2005**, *17*, 1296.
(21) (a) Hua, F.; Cui, T. Lvov, Y. M. *Nano Lett.* **2004**, *4*, 823. (b) Jiang, C.; Markutsya, S.; Tsukruk, V. V. *Adv. Mater.* **2004**, *16*, 157. (c) Tang, Z.; Kotov, N. A.; Magonov, S.; Ozturk, B. *Nat. Mater.* **2003**, *2*, 413.
(22) Podsiadlo, P.; Paternel, S.; Rouillard, J.-M.; Zhang, Z.; Lee, J.; Lee, J.-W.; Gulari, E.; Kotov, N. A. *Langmuir* **2005**, *21*, 11915.
(23) Jiang, C.; Rybak, B. M.; Markutsya, S.; Kladitis, P. E.; Tsukruk, V. V. *Appl. Phys. Lett.* **2005**, *86*, 121912.
(24) Jiang, C.; Lio, W. Y.; Tsukruk, V. V. *Phys. Rev. Lett.* **2005**, *95*, 115503.
(25) Ko, H.; Jiang, C.; Shulha, H.; Tsukruk, V. V. *Chem. Mater.* **2005**, *17*, 2490.
(26) Jiang, C.; Markutsya, S.; Shulha, H.; Tsukruk, V. V. *Adv. Mater.* **2005**, *17*, 1669.
(27) Jiang, C.; Kommireddy, D. S.; Tsukruk, V. V. *Adv. Funct. Mater.* **2006**, *16*, 27.

10.1021/cm060416x CCC: $33.50
Published on Web 05/04/2006

sealed with a flexible, freely suspended, nanoscale (85 nm thick) LbL membrane. Highly uniform photothermal behavior is also observed for a 64 × 64 array of the microscopic cavities under external thermal stimuli and IR laser illumination (Figure 1). We observed repeatable transitions from convex to concave shape of the flexible nanomembranes caused by air expansion and contraction directly associated with temperature variations. Moreover, we found that a fast optical response (time below 60 ms) to minute temperature variations (below 200 mK) is due to a buckling instability of the freely suspended nanomembranes.

Freely suspended nanomembranes were synthesized and studied as reported before (see Supporting Information).[21b,23,28−30] The half-inch 64 × 64 array of microcavities was fabricated by etching the cylindrical holes using the deep reactive etching processing.[31,32] The thermal expansion and contraction of the air inside the microcavity result in the positive/negative pressure differential and corresponding deflection of the flexible membrane which caps the silicon microcavity (Figure 1b). The scanning electron microscopy (SEM) micrographs of the silicon substrate with the microfabricated array show a high quality of cylindrical microcavities arranged in a rectangular lattice (Figure 1c). Each cylindrical pore is embedded in a rectangular area separated from one another by a trench with a 15 μm width designed to avoid the crosstalk between the neighboring cavities (Figure 1d). The smooth surface of the microfabricated array facilitates the efficient transfer of the nanoscale polymeric membrane over an entire chip. Optical and atomic force microscopy images of nanomembrane arrays are provide in Supporting Information.

Upon a change in temperature, the air thermal expansion/contraction inside the sealed microcavities causes membrane positive−negative deflections. As we demonstrated in our previous article, the permeability of the multilayer gold-containing nanomembranes under modest pressure is negligible.[23] This allows for tight sealing of the microcavities and thus a stable pressure difference under equilibrated thermal conditions. The variable deflections change light reflectance which results in a dramatic variation of the optical appearance of the array (Figure 2a−c). With the temperature varied slightly above and below room temperature where the membrane is in the planar state, the pressure inside the microcavity correspondingly becomes higher or lower than the outside pressure thus causing the flexible membrane to go through shape transformations from concave to convex as presented in the corresponding sketches (Figures 1 and 2). Such a behavior corresponds to the classical photothermal behavior of the Golay cell except that in the original design which uses metal or silicon membranes deflections are limited to nanometers and the nanomembranes studied here can easily be deflected up to 1 μm.[14] These large transformations are very reproducible and can be repeated many times

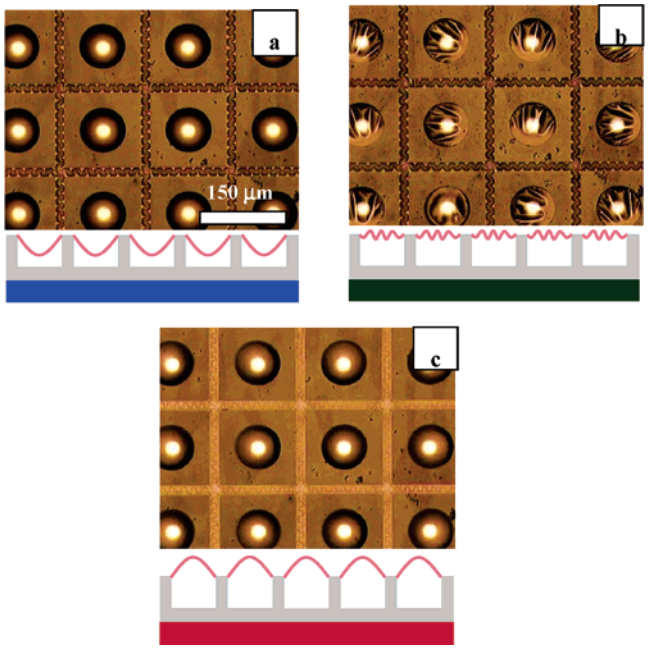

Figure 2. (a−c) Thermo-optical behavior of the freely suspended nanomembrane at various temperatures below (a), at (b), and above (c) ambient temperature, along with the corresponding cross sections of the deflected nanomembrane.

by cycling the external temperature as illustrated by real-time video (see Supporting Information).

Another notable and interesting phenomenon observed during shape transformations of the freely suspended nanomembranes was the distinguished *buckling* of flexible nanomembranes separating two uniform states (Figure 2b). Moreover, the buckling instability of the nanomembrane freely suspended across the cylindrical cavity was accompanied by instant formation of the wormlike instability of the nanomembranes along trenches (Figure 2b). These patterns are completely reversible and similar to those observed for deflected elastic plates under biaxial stresses.[33] Considering full multiple reversible changes of these buckling patterns and extremely low strains involved (below 0.1% for membranes with maximum elongation to break reaching 1%), we suggest that the observed deflections reflect elastic behavior of the nanomembranes rather than plastic deformation. These buckling patterns are associated with localized surface instabilities caused by fast stress relief during transition between two stable deformational states.[34,35]

To quantify the thermal deflection behavior of the freely suspended nanomembranes and confirm the deformational mode suggested, we carefully measured the nanomembrane deflection versus temperature with optical interferometry by analyzing the optical fringes (Figure 3a). The membrane deformation as a function of the temperature was obtained with accuracy better than ±50 nm (Figure 3b). As can be seen clearly from this plot, the membrane shows positive deflection for temperatures above room temperature (299.7 K) and negative deflection for the temperatures below room

(28) Grabar, K. C.; Freeman, R. G.; Hommer, M. B.; Natan, M. J. *Anal. Chem.* **1995**, *67*, 735.
(29) Jiang, C.; Markutsya, S.; Tsukruk, V. V. *Langmuir* **2004**, *20*, 882.
(30) Markutsya, S.; Jiang, C.; Pikus, Y.; Tsukruk, V. V. *Adv. Funct. Mater.* **2005**, *15*, 771.
(31) Yan, D.; Cheng, J.; Apsel, A. *Sens. Actuators, A* **2004**, *115*, 60.
(32) Yan, D.; Apsel, A.; Lal, A. *Smart Mater. Struct.* **2005**, *14*, 775.
(33) Audoly, B.; Roman, B.; Pocheau, A. *Eur. Phys. J. B* **2002**, *27*, 7.
(34) Stafford, C. M.; Harrison, C.; Beers, K. L.; Karim, A.; Amis, E. J.; Vanlandingham, M. R.; Kim, H.-C.; Volksen, W.; Miller, R. D.; Simonyi, E. E. *Nat. Mater.* **2004**, *3*, 545.
(35) Moon, M.-W.; Lee, K.-R.; Oh, K. H.; Hutchinson, J. W. *Acta Mater.* **2004**, *52*, 3151.

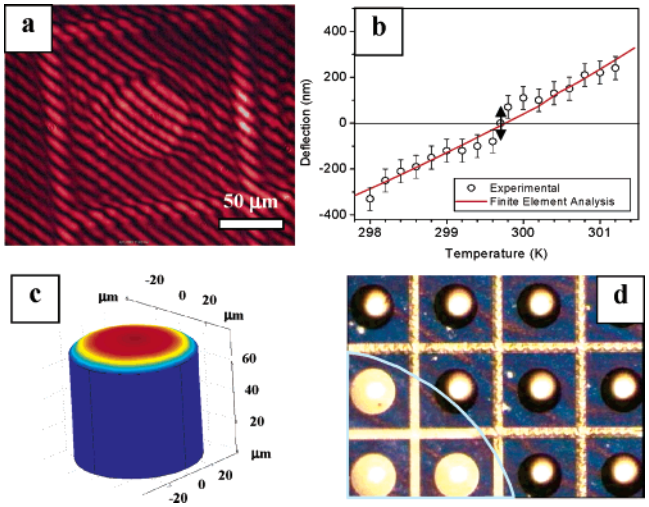

Figure 3. (a) Interference fringes for the thermally deflected membrane suspended across a microcavity, where the deformation of membrane can be monitored with the shift of fringes; (b) deflection−temperature plot for the freely suspended nanomembrane as measured from optical fringes; (c) FEA model of the cylindrical microcavity capped with a deflected flexible nanomembrane (top); and (d) direct optical detection of the edge of the NIR laser footprint (lower left-hand corner). The footprint edge is marked with a sector line.

temperature confirming optical microscopy observations (Figure 2). The slope of the deflection variation is similar for both cases (0.12 nm/mK) as can be expected for symmetrical freely suspended membranes.[23] However, a large abrupt change in the membrane deflection was observed in the vicinity of the room temperature which can be associated with buckling instability observed with the optical microscopy (Figure 2). The membrane deflection changed by 200 nm within a narrow temperature interval of 200 mK (Figure 3b). These changes are very fast and are completed within 60 ms as estimated from frame-by-frame video (see Supporting Information). The effective thermal sensitivity in this narrow interval reaches 1 nm/mK, which exceeds current values for silicon membranes 10-fold.[14] Moreover, this value is much higher than that achieved for best-performing uncooled microcantilever sensors.[36,37]

To verify if the pressure variation generated by air thermal expansion−contraction within sealed microcavities can be responsible for the nanomembrane deflection observed we simulated the thermal behavior of a single microcavity with a freely suspended flexible nanomembrane (Figure 3c). The three-dimensional finite element analysis (FEA) model shows an overall deformation of the sealed microcavity with the largest variation achieved at the center of the flexible membrane under air pressure induced by a 2 K temperature differential. Plotting the deformation of the membrane versus temperature generates a linear graph (Figure 3b). This plot fits nicely the observed deflection for a whole temperature range except for a discontinuity around the room temperature related to the buckling instability, which is not accounted by FEA simulation conducted in the linear elastic regime. Therefore, this simulation confirms that the air pressure variation within the sealed microcavities can cause the elastic membrane deflections observed experimentally.

The photothermal response of a flexible nanomembrane array was also studied under direct near-infrared (NIR) radiation (Figure 3d). If a portion of the membrane microcavity array was illuminated (the lower left-hand corner in Figure 3d), we observed clear localized change in optical reflection caused by localized minute heating. Moreover we did not observe cross-talking between neighboring cells of 80 μm in diameter separated by trenches indicating that these microcavity arrays can be excellent candidates for high-resolution, highly sensitive IR microimaging devices.

In conclusion, we observed the photothermal phenomenon for a single microscopic cavity sealed with a flexible, freely suspended nanoscale polymeric membrane with encapsulated gold nanoparticles. Moreover, we demonstrated that the photothermal behavior can be scaled up to a large (64 × 64) array of the microscopic cavities, thus creating an efficient microscopic thermal imaging array operating at room temperature. We observed reproducible, multiple transitions from convex to concave shape of the flexible nanomembranes caused by air thermal expansion and contraction. We found an interesting buckling instability phenomenon, which facilitates a fast optical response to minute temperature variations and results in outstanding thermal sensitivity exceeding 10-fold the known value for thermal microsensors. We believe that these results and direct demonstration of the passive visualization of the NIR laser beam with high spatial resolution (below 40 μm) pave the way toward a new generation of uncooled, miniature, ultrasensitive, photothermal imagers for a wide range of microsensing applications. Enhancing the sensitivity, affordability, and further miniaturization of passive and uncooled IR microsensors is critical for both military and civilian applications ranging from reconnaissance and targeting to medical imaging and fingerprint identification.[38,39] We suggest that further refining of this design would allow achieving the thermal sensitivity of solid-state cooled IR detectors which is currently around 10 mK.[40,41]

Acknowledgment. The authors thank Dr. Dong Yan from Agiltron Incorporated for substrate fabrication. This work is supported by AFOSR, F496200210205, F49620-03-1-0273, W31P4Q-05-C-R029, FA9550-04-C-0099, and NSF-CTS-0506832 Grants.

Supporting Information Available: Experimental details and characterization of nanomembrane arrays (PDF) and real-time video of the thermo-optical behavior of the microcavity array (MPEG). This material is available free of charge via the Internet at http://pubs.acs.org.

CM060416X

(36) (a) Lin, Y.-H.; McConney, M.; LeMieux, M. C.; Peleshanko, S.; Jiang, C.; Singamaneni, S.; Tsukruk, V. V. *Adv. Mater.* **2006**, *18*, 1157. DOI: 10.1002/adma.200502232. (b) LeMieux, M. C.; McConney, M.; Lin, Y.-H.; Singamaneni, S.; Jiang, H.; Bunning, T. J.; Tsukruk, V. V. *Nano Lett.* **2006**, *6*, 730.
(37) Corbeil, J. L.; Lavrik, N. V.; Rajia, S. *Appl. Phys. Lett.* **2002**, *81*, 1306.
(38) Kayes, R. J. *Optical and Infrared Detectors;* Springer-Verlag: Berlin, 1977.
(39) Rogalski, A. *Prog. Quantum Elect.* **2003**, *27*, 59.
(40) Zhao, Y.; Mao, M.; Horowitz, R., Majumdar, A.; Varesi, J.; Norton, P.; Kitching, J. *J. Microelectromechanical Systems* **2002**, *11*, 136.
(41) Datskos, P. G.; Lavrik, N. V.; Rajic, S. *Rev. Sci. Instrum.* **2004**, *75*, 1134.